APPLIED AND ENVIRONMENTAL MICROBIOLOGY, Jan. 2010, p. 560–565 Vol. 76, No. 2
0099-2240/10/$12.00 doi:10.1128/AEM.02205-09

Iron Sources Used by the Nonpathogenic Lactic Acid Bacterium *Lactobacillus sakei* as Revealed by Electron Energy Loss Spectroscopy and Secondary-Ion Mass Spectrometry▽†

Philippe Duhutrel,[1] Christian Bordat,[2] Ting-Di Wu,[3,4] Monique Zagorec,[1] Jean-Luc Guerquin-Kern,[3,4] and Marie-Christine Champomier-Vergès[1]*

Unité Flore Lactique et Environnement Carné, UR309, INRA, Domaine de Vilvert, F-78350 Jouy en Josas, France[1]; Unité Nurélice, UR909, INRA, Domaine de Vilvert, F-78350 Jouy en Josas, France[2]; U 759 INSERM, F-91405 Orsay, France[3]; and Institut Curie, Laboratoire de Microscopie Ionique, F-91405 Orsay, France[4]

Received 11 September 2009/Accepted 9 November 2009

Lactobacillus sakei **is a lactic acid bacterium naturally found on meat. Although it is generally acknowledged that lactic acid bacteria are rare species in the microbial world which do not have iron requirements, the genome sequence of *L. sakei* 23K has revealed quite complete genetic equipment dedicated to transport and use of this metal. Here, we aimed to investigate which iron sources could be used by this species as well as their role in the bacterium's physiology. Therefore, we developed a microscopy approach based on electron energy loss spectroscopy (EELS) analysis and nano-scale secondary-ion mass spectrometry (SIMS) in order to analyze the iron content of *L. sakei* cells. This revealed that *L. sakei* can use iron sources found in its natural ecosystem, myoglobin, hemoglobin, hematin, and transferrin, to ensure long-term survival during stationary phase. This study reveals that analytical image methods (EELS and SIMS) are powerful complementary tools for investigation of metal utilization by bacteria.**

Most living organisms have requirements for iron, an element which is indispensable for many cellular processes. Its role in infection and virulence processes in pathogenic bacteria has also been evidenced (reference 11 and references therein). In the environment, iron cannot be used readily by bacteria because of its insolubility. In response to iron deprivation, microorganisms have thus developed sophisticated strategies in order to capture and sequestrate iron. Gram-negative and Gram-positive species generally synthesize extracellular siderophores, low-molecular compounds with very high affinity for ferric iron, and specific membrane receptors able to internalize iron-siderophore complexes (40). Some bacteria with absolute iron requirements, such as *Pseudomonas fragi*, a meat-borne species which does not produce siderophores, or the pathogenic species *Staphylococcus aureus*, which produces only three different siderophores, are able to use iron-siderophore complexes produced by other bacterial species sharing their environment (10, 36). In animals, heme constitutes the major iron source and is found in hemoproteins, such as hemoglobin and myoglobin. Bacteria can also gain free heme from proteolysis or oxidation of free hemoglobin issued from red blood cells. Other mammalian iron sources can be found in nonheminic iron storage and transport proteins, such as transferrin or lactoferrin.

Until recently, lactic acid bacteria were generally considered to be a rare bacterial group having no iron requirement (7, 41). No growth differences were noticed when different lactic acid bacterium species were tested in either iron-depleted or iron-supplemented media, and attempts to characterize siderophore production by these species were unsuccessful (22, 34). Recently, nonribosomal peptide synthesis pathways have been detected with the genomes of two *Lactococcus lactis* vegetal isolates (37). The authors of that study suggest that this could account for siderophore production as it exists in other bacteria (11), but this remains to be experimentally proven. One species, *Lactobacillus johnsonii*, exhibits iron requirements when inosine and uracil are supplied as the sole nucleotide sources in a chemically defined medium (15). Heme acquisition in *Lactococcus lactis* has been reported and is associated with the ability of the species to undergo respiration (13). But iron per se is still considered to be dispensable for these species, and heme is considered a heme source rather than an iron source. Genome sequences of several lactic acid bacteria have revealed that some species harbor genetic equipment involved in iron transport (31). This is the case in *Lactobacillus sakei*, a lactic acid bacterium particularly well adapted to meat, in which it becomes the predominant flora. Its genome has revealed some specific features that could account for its high adaptation to meat, including several putative iron transport systems and three iron-dependent transcriptional regulators belonging to the Fur family (8). *L. sakei* lacks classical respiratory cytochromes and is devoid of heme biosynthesis machinery, but a heme-dependent catalase has previously been reported (20, 26). The genome sequence of strain 23K showed the presence of putative cytochrome b_5 (8) and a mutated cytochrome P450 gene, this latter gene being intact in some other *L. sakei* strains (9). This equipment may indicate that iron and/or heme is transported into *L. sakei* cells.

* Corresponding author. Mailing address: Unité Flore Lactique et Environnement Carné, UR309, INRA, Domaine de Vilvert, F-78350 Jouy en Josas, France. Phone: 33 (0) 134 65 22 92. Fax: 33 (0) 1 34 65 21 05. E-mail: marie-christine.champomier-verges@jouy.inra.fr.

† Supplemental material for this article may be found at http://aem.asm.org/.

▽ Published ahead of print on 20 November 2009.

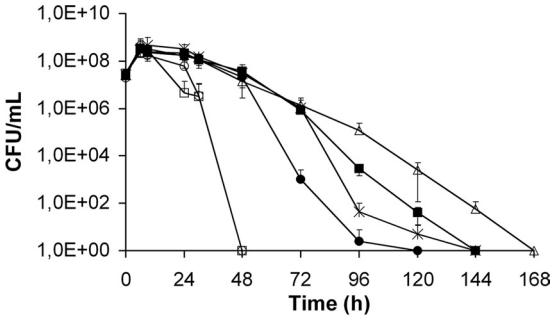

FIG. 1. Growth and survival of *L. sakei* 23K in MCD medium supplemented with various iron sources. Open squares, control; open circles, $FeCl_3$, 40 μM; open triangles, hematin, 40 μM; crosses, hemoglobin, 10 μM; full squares, myoglobin, 40 μM; full circles, h-transferrin, 5 μM. Iron source concentrations were calculated to ensure the same final Fe concentration. h-Transferrin concentrations ranging from 1 to 20 μM were tested, but no difference was observed between 5 and 20 μM, so the 5 μM concentration was selected.

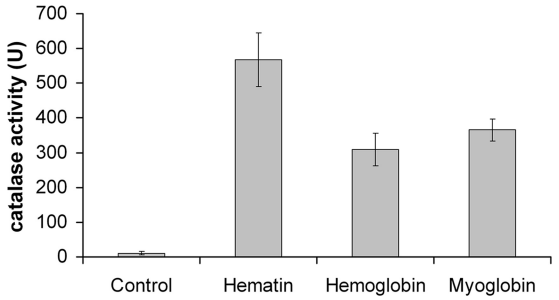

FIG. 2. Histogram representing catalase activity of *L. sakei* cells grown in MCD medium supplemented with heminic compounds (control, hematin, 40 μM; hemoglobin, 10 μM; myoglobin, 40 μM). Catalase activity is expressed as micromoles H_2O_2 consumed per minute and per mg protein.

Numerous methods have been used to study metal-microorganism interactions. An extensive review of methodological approaches was done in 1997 (1). Recently, mapping of organic polymers and the redox iron status of bacterial extracellular matrixes have been studied by scanning transmission X-ray microscopy (21, 32). Electron energy loss spectroscopy (EELS) and/or electron spectroscopic imaging (ESI) techniques have successfully been used in eukaryotic tissue investigation in order to visualize ultrastructural localization of elements such as calcium, phosphorous, oxygen, nitrogen, zinc, copper, other light elements, and also iron (3, 5, 6, 17, 23–25, 39). EELS also allowed identification of phosphorus and thus DNA in an extracellular matrix produced by a Gram-negative bacterial isolate involved in biofilm formation (2). The nitrogen distribution map created through EELS image analysis allowed the localization of cyanophin, a cyanobacterial protein known for functioning as temporary nitrogen, carbon, and energy stock (27). Information on the cellular status of metals in bacteria is difficult to obtain, since conventional preparations used for electron-microscopic observations can alter structures, relocate, and/or remove metal ions and probably other labile cytoplasmic constituents when processing at room temperature (16). Secondary-ion mass spectrometry (SIMS) has been used for a couple of years to investigate the isotopic composition of microorganisms (33) and recently to identify uncultured microorganisms in complex ecosystems by using species-specific oligonucleotide probes (29). Here, we developed an analytical correlative imaging approach based on a combination of EELS and SIMS, which revealed that growth of *L. sakei* in the presence of heminic compounds or transferrin leads to iron accumulation in cells, which is correlated with a longer survival during stationary phase.

MATERIALS AND METHODS

Bacterial strain and growth conditions. *L. sakei* 23K (8) was propagated on MRS medium (12) at 30°C. For physiological studies the chemically defined medium MCD (28) supplemented with 0.5% (wt/vol) glucose was used. MCD medium contains no iron sources but contains possible traces of iron coming from various components or distilled water. Incubation was performed at 30°C with stirring at 70 rpm. Cell growth and viability were followed by measuring the optical density at 600 nm (OD_{600}) on a visible spectrophotometer (Secomah) and by the determination of the number of CFU ml^{-1} after plating serial dilutions of samples on MRS agar. Plates were incubated under aerobiosis at 30°C for 30 h. All the measurements were performed in at least three independent assays. When needed, media were supplemented with freshly prepared filtered solutions to obtain final concentrations of either 40 μM $FeCl_3$ (Merck), 40 μM $FeSO_4$ (Merck), 40 μM hematin (Sigma), 10 μM hemoglobin (Sigma), 40 μM myoglobin (Sigma), 5 μM bovine holo-transferrin (h-transferrin; Sigma), 2.5 μM ferrichrome (Sigma), 1 μM lactoferrin (Sigma), 40 μM desferrioxamin (Desferal; Sigma) iron saturated with $FeCl_3$, or 50 μM ferri tri-sodium citrate (Merck). Iron depletion was obtained by addition of *O*-phenanthroline (Sigma) or 2,2 dipyridyl (Sigma) at 200 μM or at 2 to 4 mM in liquid medium or agar medium, respectively.

Catalase activity determination (adapted from the method of Sinha [38]). Cells cultivated for 8 h in MCD medium supplemented with hematin, hemoglobin, or myoglobin were collected by centrifugation (3,300 x *g*) for 10 min at 4°C, rinsed twice in sodium phosphate buffer (0.1 M, pH 7.0), and resuspended in the same buffer at an OD_{600} of up to 25. Cell suspensions (700 μl) were added to 500-mg glass beads (0.1-mm diameter; BioSpec Products) and disrupted on a FastPrep apparatus (FP120; Bio101 Savant) by shaking twice for 20 s at speed 5, with a cooling step between of 2 min on ice. After centrifugation for 10 min at 15,000 × *g*, the protein concentration was measured in the supernatant using the Bradford method according to the manufacturer's instructions (Coomassie protein assay reagent; Pierce Biotechnology, Rockford, IL). Catalase activity was determined with cell extract aliquots containing 100-μg proteins incubated in the presence of 5 ml sodium phosphate buffer (0.1 M, pH 7.0) and 4 ml H_2O_2 (0.2 M). At 1, 3, 5, 8, and 10 min, 1-ml aliquots were removed and mixed to 2 ml (potassium dichromate [50 g $liter^{-1}$]-acetic acid [1:2, vol/vol]), then boiled for 10 min before the OD_{570} was measured. Results are expressed as micromoles H_2O_2 consumed per minute and per mg of proteins. Three independent assays were performed, and results are expressed as mean ± standard deviation.

Sample preparation for EFTEM and SIMS analysis. Cells grown for 8 h and 30 min (OD_{600} of ~1.4) in MCD medium supplemented with various iron sources were harvested by gentle centrifugation at room temperature. A small amount of bacterial pellet was quickly pushed in a spacer ring fixed with a double-side rubber onto the specimen holder of a cryofixation device (Metal-Mirror cryofixation system MM80 E; Leica, Vienna, Austria) and impacted onto a liquid nitrogen-cooled gold-coated copper block. The freeze substitution process in pure dry acetone at −89°C for 3 days in a freeze substitution device (AFS, Leica, Vienna, Austria), progressive infiltration in Spurr resin, a polymerization step, and sectioning (Ultracut S microtome; Leica, Vienna, Austria) were performed as previously described (4). Thin sections (50 nm thick) collected on unfilmed grids were examined unstained on an energy-filtered transmission electron microscope (EFTEM), a CEM 902 Carl Zeiss (Oberkochen, Germany) equipped with a charge-coupled-device camera, Mega View III FW (Olympus Soft Imaging Solutions, Münster, Germany), located at the Platform MIMA2 (INRA, Jouy en Josas, France). Acquisition, recording, and treatment of data were obtained with graphical interface iTEM (Soft Imaging Company, Münster, Germany).

EELS analysis procedure. In an electron microscope, electrons which have been scattered in the specimen lose element-specific energies. These electrons can be detected as a function of the energy lost through the specimen by the means of an energy filter that permits recording element distribution images (ESI) and spectra (EELS). Element-specific signals (elemental edges) are su-

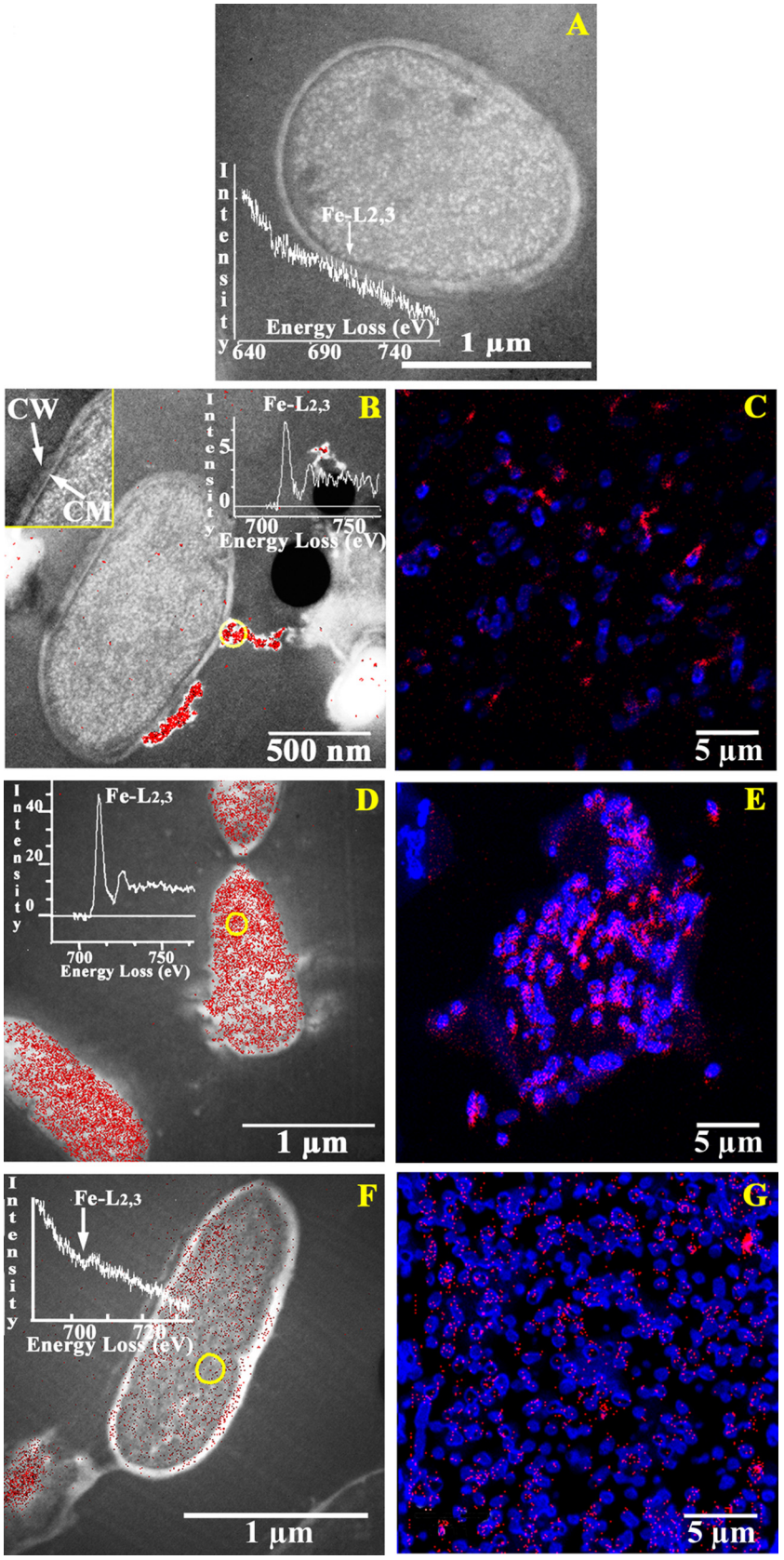

FIG. 3. Iron mapping of *L. sakei* cells cultivated in MCD medium supplemented with various iron sources: no iron (A); ferrioxamin, 40 μM (B and C); myoglobin, 40 μM (D and E); and h-transferrin, 5 μM (F and G). ESI images obtained using EFTEM (cell scale) (panels A, B, D, and

perimposed on a falling background. In this study we used parallel EELS (PEELS) as an alternative to the EELS technique to identify iron; in this technique an image of the spectrum is recorded by the camera and the resulting spectrum represents the distribution of image pixel intensity as a function of energy loss. iTEM software allowed us to remotely control the microscope and camera for data acquisitions and to analyze energy-filtered images and spectra. The ESI technique produces highly resolved element mapping of preparations over relatively large areas, and the PEELS technique, suitable for a fast screening of spectra, allows chemical analysis with good spatial resolution. Comparison of ESI maps and PEELS spectra recorded on the same analyzed region avoids false image distribution due to possible local changes in section thickness and allows identification of weak edges. In this study, iron was identified by the Fe-$L_{2,3}$ edge at 708 eV (35). Images (516 by 516 by 8, binning [x/y] of 2x) were recorded by the camera using iTEM software facilities. An iron map was obtained by subtracting a modeled background using the three-window power law method (14). Detailed descriptions of the method are given elsewhere (35). An additional image at an energy loss (ΔE) of 250 eV (structure-sensitive image) below the C-K edge, which allows examination of very thin unstained sections, was obtained at the same time. At this value, the contrast image is inverted, carbon contribution is eliminated, and cellular details are clearly visible. The calculated element map, arbitrarily colored, was superimposed onto the corresponding structure-sensitive image. For PEELS acquisition, the image of the EELS spectrum was recorded by the camera, with an energy range of 140 eV centered at the energy loss of the Fe-$L_{2,3}$ edge (708 eV). Background subtraction was performed using the iTEM software facilities, and the calculated background according to the power law of Egerton (14) was subtracted from experimental spectra. If EFTEM analysis allows iron detection at a nano-scale range, this analytical technique is restricted to a limited field of view (about 3 μm by 3 μm), therefore studying numerous bacteria to get information on a large cell population would be time consuming.

SIMS imaging. SIMS allows direct identification of chemical elements with high sensitivity and specificity (18) and can be applied to visualizing the elemental distribution (chemical mapping) of a large area (raster of up to 100 μm) to get an overview of a few tens of cells in addition to highly resolved EFTEM maps. Dynamic SIMS imaging was performed using a NanoSIMS-50 ion microprobe (CAMECA, France) operating in scanning mode. The primary ion beam was generated from either a cesium source (Cs^+) or an oxygen source (O^-) for, respectively, negative or positive secondary-ion analysis. The instrument is equipped with a magnetic spectrometer using a parallel detection system with the capacity to acquire simultaneously up to five species, which ensures a perfect colocalization between recorded images. In this study, images for CN^-, P^-, and S^- were acquired simultaneously using the Cs^+ primary beam to characterize the cell distribution. Concerning the detection of iron, Fe^- emission using the Cs^+ beam (electronic affinity, EA of 0.16 eV) provides extremely low sensitivity. As an alternative, several tests have been carried out by detecting FeO^- (EA of 1.5 eV). However, the sensitivity is still quite low, and only aggregated iron could be analyzed in this way. The magnetic field was set to detect the heaviest mass (in the present study, $^{56}Fe^{16}O^-$ with the Cs source) on one of the largest radius detectors. The other movable detectors were positioned to detect $^{12}C^{14}N^-$ and $^{31}P^-$. For typical experiments, the primary ion intensity was up to 6 pA. The probe was stepped over the sample in a 256-by-256-pixel raster of 100 to 30 μm to generate secondary-ion images. The typical dwell time was 20 ms per pixel. As Fe can be more favorably detected as Fe^+, imaging was also carried out using the O^- beam on samples showing a low and more homogeneous iron distribution. Sections were first examined using the O^- beam to record $^{40}Ca^+$ and $^{56}Fe^+$ maps ($^{40}Ca^+$ is used to characterize the cell distribution). The typical acquisition duration was then extended to about 50 ms per pixel for the detection of positive secondary-ion species $^{40}Ca^+$ and $^{56}Fe^+$ at a much lower intensity (3 pA). Recording was then performed using multiframe mode (accumulation of 10 frames with 5 ms per pixel for each) in order to prevent structure deformation because of the erosion of primary ions. The same regions of interest were then analyzed using the Cs^+ beam to acquire $^{12}C^{14}N^-$, $^{31}P^-$ and $^{32}S^-$ images in a separate run. As the two sets of images were recorded sequentially, care has been taken to minimize the shift between the two sets of images during image acquisition. Furthermore, image processing using ImageJ software (W. S. Rasband, 1997–2000, National Institutes of Health, Bethesda, MD [http://rsb.info. nih.gov/ij/]), with a homemade plug-in, was performed to obtain proper colocalization of the observed structures on the processed maps for all of the ion species.

RESULTS AND DISCUSSION

***L. sakei* showed enhanced survival during stationary phase when grown in the presence of heminic compounds or transferrin.** We first aimed at analyzing *L. sakei* behavior in the presence of iron. As previously claimed for several lactic acid bacteria, neither iron deprivation nor iron supplementation modified growth of *L. sakei* 23K (data not shown). Iron deprivation was obtained by adding common iron chelators: *O*-phenanthroline (200 μM to 4 mM), 2,2 dipyridyl (200 μM to 4 mM), or Desferal (200 μM). No effect of Desferal or 2,2 dipyridyl was observed on growth in either solid or liquid media. A total growth inhibition was observed when *O*-phenanthroline was added, but this inhibition was not suppressed by subsequent iron supplementation, indicating an intrinsic toxicity of *O*-phenanthroline, independent from an iron privation effect, as previously reported for lactic acid bacteria (30). None of the iron source supplementations tested (free-iron forms $FeSO_4$ or $FeCl_3$; siderophore-complexed iron ferrichrome, ferrioxamin, and ferri-citrate; and iron forms present in the meat environment, such as hematin, hemoglobin, myoglobin, h-transferrin, and lactoferrin) resulted in any significant effect on growth (data not shown). This indicates that this metal is dispensable for *L. sakei* growth. In contrast, survival was highly enhanced during stationary phase when cells were grown in the presence of heminic compounds (hematin, myoglobin, and hemoglobin), with cells being able to survive up to 144 to 168 h (Fig. 1). The most pronounced effect was observed in the presence of hematin. An intermediate phenotype was observed when h-transferrin was added to the medium. In fact, this compound led to a better survival than the one observed with the control, even though it was less than that with heminic compounds. These results confirm that iron is dispensable for *L. sakei* growth, as mentioned in the literature (34), but they clearly indicate that iron sources present in the meat environment highly benefit *L. sakei* by sustaining long-term survival.

Catalase activity is correlated with enhanced survival in the presence of heme. As *L. sakei* is known for possessing a heme-dependent catalase (20, 26), even though it is deficient in a heme biosynthesis pathway, we measured this activity in cells grown in the presence of different heme sources. As shown in Fig. 2, growth in the presence of hematin, hemoglobin, or myoglobin resulted in measurable catalase activity in *L. sakei* cells, indicating that this species is able to get heme from the

F). A filtered image at 250 eV (inverted contrast) allows the morphology to be observed. Bacterium ultrastructure is clearly visible; ribosomes nonhomogeneously distributed are recognizable (panels A and B especially). Magnified insert in panel B shows a small portion of membranes with cytoplasmic membrane (CM) and cell wall (CW) well conserved. The iron map, in red, is superimposed on the 250-eV image. White inserts show experimental PEELS spectra (panels A and F) or background-corrected Fe-$L_{2,3}$ edges (panels B and D). Yellow circles represent the area for PEELS acquisitions. Unstained sections. SIMS images (population scale) (panels C, E, and G). SIMS has the capacity to analyze a larger field (here 30 μm) and then complementing and generalizing the ESI information obtained for single cells. Images were obtained by superimposing two sets of images: the iron ($^{56}Fe^{16}O^-$ for panel C and $^{56}Fe^+$ for panels E and G) distribution in red and the $^{12}C\ ^{14}N^-$ distribution in blue, which gives information on cell distribution.

hemoproteins hemoglobin and myoglobin. Significantly higher catalase activity was observed with cells grown in the presence of hematin and is correlated with longer survival during stationary phase. The survival in the presence of heminic compounds cannot be attributed to respiration, as described for *L. lactis* (13), since *L. sakei* lacks respiratory cytochromes (8), but could be attributed to the dismutation of hydrogen peroxide by the catalase. The survival in the presence of h-transferrin relies on the effect of iron per se and not on heme. Such an effect of iron and the ability to get it from h-transferrin was unexpected and had not yet been observed with lactic acid bacteria. Additionally, we could not detect any catalase activity in cells grown in the presence of h-transferrin. Taking all these results into consideration, we cannot rule out that heme per se is also used as an iron source.

Heminic iron sources and transferrin are transported into *L. sakei* cells. Our strategy to evaluate the intracellular iron content of *L. sakei* cells grown in the presence of various iron sources was to develop an electron microscopy-based method. From the same cell preparation we performed both EELS to get an iron map at nanometer range for single cells and NanoSIMS in order to visualize iron within the whole-cell population. As no precise quantification could be performed in any of the techniques, the combination of both approaches revealed to be efficient in evaluating the iron content of cellular populations, and the two techniques clearly appear complementary. Conventional procedures for sample preparation for EFTEM analysis usually include, prior to resin embedding, chemical fixations and dehydrations in solutions with increasing organic solvent content that produce extractions or displacements of loosely bound elements (19). To avoid these artifacts, we used physical fixation (cryofixation) and cryosubstitution prior to the necessary embedding in a resistant resin. Cell structure conservation of such preparations was checked by TEM observations. We detected the presence of iron inside cellular structures, confirming that cell integrity had been kept, which ensured intracellular conservation of elements. EFTEM analyses at the subcellular level were confirmed by NanoSIMS analysis in corresponding areas but in larger zones. Several observations were made with the whole-cell preparation, and we present here representative images for EFTEM and SIMS analysis (Fig. 3). Clear differences were observed for the iron content of cells grown on various iron sources. Cells grown in the absence of exogenous iron sources did not show any iron signal in their cytoplasm (Fig. 3A). Cells grown in the presence of $FeCl_3$ or ferrioxamin revealed a weak iron signal (iron content near the limit of detection) in the cytoplasm, whereas extracellular clusters exhibited a strong signal, indicating that iron does not enter the cells as shown for ferrioxamin grown cells (Fig. 3B and C). We detected the presence of iron in *L. sakei* cells grown in the presence of myoglobin, hematin, and hemoglobin, characterized by a strong signal from cytoplasm (Fig. 3D and E; see also Fig. S1 in the supplemental material). Likewise, we observed an iron signal in the cytoplasm of cells grown in the presence of h-transferrin (Fig. 3F and G), though it was less strong than the one observed with heminic compounds. It seems that iron accumulation in *L. sakei* cells varies according to iron source supply, with heminic compounds, such as heme, hemoglobin, or myoglobin, being preferential iron sources for *L. sakei*. These differences in iron cellular contents are correlated with bacterial survival. Indeed, a lower iron content was observed with transferrin, a growth condition for which survival during stationary phase was less improved than with the heminic iron sources. In all cases, the use of SIMS confirmed the presence of iron at the population level, strengthening information obtained for single cells. This was characterized by the colocalization of ^{+56}Fe and ^{-}CN (cell structure) secondary-ion images. We also observed a nonhomogeneous signal within cells, which could be due to differences in the physiological statuses of cells within the population.

In conclusion, this study provides the first evidence for both heme and iron utilization by *L. sakei* for its survival. This utilization seems restricted to iron sources present in the meat environment, such as myoglobin, hemoglobin, and transferrin, confirming the tight adaptation of this species to meat. This enlightens us about the functions critical for its adaptation and that ensure the competitiveness of this meat-borne lactic acid bacterium. In addition, we have developed a novel complementary use of EELS and SIMS, which represents a promising experimental approach offering the possibility of detecting intracellular iron in bacteria. This should be of interest in particular to studies of pathogens known for having higher iron requirements and should open new fields for element investigation of bacteria.

ACKNOWLEDGMENTS

We thank Platform MIMA2, INRA, Jouy en Josas, France.

P. Duhutrel is recipient of a grant from the French Ministère de la Recherche.

REFERENCES

1. **Beveridge, T. J., M. N. Hughes, H. Lee, K. T. Leung, R. K. Poole, I. Savvaidis, S. Silver, and J. T. Trevors.** 1997. Metal-microbe interactions: contemporary approaches. Adv. Microb. Physiol. **38:**177–243.
2. **Bockelmann, U., H. Lunsdorf, and U. Szewzyk.** 2007. Ultrastructural and electron energy-loss spectroscopic analysis of an extracellular filamentous matrix of an environmental bacterial isolate. Environ. Microbiol. **9:**2137–2144.
3. **Bordat, C., A. Constans, O. Bouet, I. Blanc, C. L. Trubert, R. Girot, and G. Cournot.** 1993. Iron distribution in thalassemic bone by energy-loss spectroscopy and electron spectroscopic imaging. Calcif. Tissue Int. **53:**29–37.
4. **Bordat, C., and J. L. Guerquin-Kern.** 2008. Cryo-preparation procedures for elemental imaging by SIMS and EFTEM, p. 499–536. *In* A. Cavalier, D. Spehner, and B. Humbel (ed.), Handbook of cryo-preparation methods for electron microscopy, vol. 7. CRC Press, Boca Raton, FL.
5. **Bordat, C., J. L. Guerquin-Kern, M. Lieberherr, and G. Cournot.** 2004. Direct visualization of intracellular calcium in rat osteoblasts by energy-filtering transmission electron microscopy. Histochem. Cell Biol. **121:**31–38.
6. **Bordat, C., M. Sich, F. Rety, O. Bouet, G. Cournot, C. A. Cuenod, and O. Clément.** 2000. Distribution of iron oxide nanoparticles in rat lymph nodes studied using electron energy loss spectroscopy (EELS) and electron spectroscopic imaging (ESI). J. Magn. Reson. Imaging **12:**505–509.
7. **Bruyneel, B., M. Vandewoestyne, and W. Verstraete.** 1989. Lactic acid bacteria: microorganisms able to grow in the absence of available iron and copper. Biotechnol. Lett. **11:**401–406.
8. **Chaillou, S., M. C. Champomier-Vergès, M. Cornet, A. M. Crutz-Le Coq, A. M. Dudez, V. Martin, S. Beaufils, E. Darbon-Rongère, R. Bossy, V. Loux, and M. Zagorec.** 2005. The complete genome sequence of the meat-borne lactic acid bacterium *Lactobacillus sakei* 23K. Nat. Biotechnol. **23:**1527–1533.
9. **Chaillou, S., M. Daty, F. Baraige, A. M. Dudez, P. Anglade, R. Jones, C. A. Alpert, M. C. Champomier-Vergès, and M. Zagorec.** 2009. Intraspecies genomic diversity and natural population structure of the meat-borne lactic acid bacterium *Lactobacillus sakei*. Appl. Environ. Microbiol. **75:**970–980.
10. **Champomier-Vergès, M. C., A. Stintzi, and J. M. Meyer.** 1996. Acquisition of iron by the non-siderophore-producing *Pseudomonas fragi*. Microbiology **142:**1191–1199.
11. **Crosa, J. H., and C. T. Walsh.** 2002. Genetics and assembly line enzymology of siderophore biosynthesis in bacteria. Microbiol. Mol. Biol. Rev. **66:**223–249.

12. **De Man, J. C., M. Rogosa, and M. E. Sharpe.** 1960. A medium for the cultivation of *Lactobacilli*. J. Appl. Bacteriol. **23:**130–135.
13. **Duwat, P., S. Sourice, B. Cesselin, G. Lamberet, K. Vido, P. Gaudu, Y. Le Loir, F. Violet, P. Loubière, and A. Gruss.** 2001. Respiration capacity of the fermenting bacterium *Lactococcus lactis* and its positive effects on growth and survival. J. Bacteriol. **183:**4509–4516.
14. **Egerton, R. F.** 1989. Electron energy-loss spectroscopy in the electron microscope. Plenum Press, New York, NY.
15. **Elli, M., R. Zink, A. Rytz, R. Reniero, and L. Morelli.** 2000. Iron requirement of *Lactobacillus* spp. in completely chemically defined growth media. J. Appl. Microbiol. **88:**695–703.
16. **Eltsov, M., and B. Zuber.** 2006. Transmission electron microscopy of the bacterial nucleoid. J. Struct. Biol. **156:**246–254.
17. **Grohovaz, F., M. Bossi, R. Pezzati, J. Meldolesi, and F. T. Tarelli.** 1996. High resolution ultrastructural mapping of total calcium: electron spectroscopic imaging electron energy loss spectroscopy analysis of a physically/chemically processed nerve-muscle preparation. Proc. Natl. Acad. Sci. U. S. A. **93:**4799–4803.
18. **Guerquin-Kern, J.-L., T.-D. Wu, C. Quintana, and A. Croisy.** 2005. Progress in analytical imaging of the cell by dynamic secondary ion mass spectrometry (SIMS microscopy). Biochim. Biophys. Acta **1724:**228–238.
19. **Hayat, M.** 2000. Principles and techniques of electron microscopy: biological applications, 4th ed, p. 377–406. Cambridge University Press, Cambridge, United Kingdom.
20. **Hertel, C., G. Schmidt, M. Fischer, K. Oellers, and W. P. Hammes.** 1998. Oxygen-dependent regulation of the expression of the catalase gene *katA* of *Lactobacillus sakei* LTH677. Appl. Environ. Microbiol. **64:**1359–1365.
21. **Hunter, R. C., A. P. Hitchcock, J. J. Dynes, M. Obst, and T. J. Beveridge.** 2008. Mapping the speciation of iron in *Pseudomonas aeruginosa* biofilms using scanning transmission X-ray microscopy. Environ. Sci. Technol. **42:** 8766–8772.
22. **Imbert, M., and R. Blondeau.** 1998. On the iron requirement of lactobacilli grown in chemically defined medium. Curr. Microbiol. **37:**64–66.
23. **Jeanguillaume, C.** 1987. Electron-energy loss spectroscopy and biology. Scanning Microsc. **1:**437–450.
24. **Jeanguillaume, C., M. Tence, P. Trebbia, and C. Colliex.** 1983. Electron-energy loss chemical mapping of low Z elements in biological sections. Scan. Electron Microsc. 745–756.
25. **Jonas, L., G. Fulda, T. Salameh, W. Schmidt, G. E. Kroning, U. T. Hopt, and H. Nizze.** 2001. Electron microscopic detection of copper in the liver of two patients with morbus Wilson by EELS and EDX. Ultrastruct. Pathol. **25:** 111–118.
26. **Knauf, H. J., R. F. Vogel, and W. P. Hammes.** 1992. Cloning, sequence, and phenotypic expression of *katA*, which encodes the catalase of *Lactobacillus sakei* LTH677. Appl. Environ. Microbiol. **58:**832–839.
27. **Koop, A., I. Voss, A. Thesing, H. Kohl, R. Reichelt, and A. Steinbuchel.** 2007. Identification and localization of cyanophycin in bacteria cells via imaging of the nitrogen distribution using energy-filtering transmission electron microscopy. Biomacromolecules **8:**2675–2683.
28. **Lauret, R., F. Morel-Deville, F. Berthier, M. C. Champomier-Vergès, P. Postma, S. D. Ehrlich, and M. Zagorec.** 1996. Carbohydrate utilization in *Lactobacillus sakei*. Appl. Environ. Microbiol. **62:**1922–1927.
29. **Li, T., T. D. Wu, L. Mazeas, L. Toffin, J. L. Guerquin-Kern, G. Leblon, and T. Bouchez.** 2008. Simultaneous analysis of microbial identity and function using NanoSIMS. Environ. Microbiol. **10:**580–588.
30. **MacLeod, R. A.** 1952. The toxicity of *o*-phenanthroline for lactic acid bacteria. J. Biol. Chem. **197:**751–761.
31. **Makarova, K., A. Slesarev, Y. Wolf, A. Sorokin, B. Mirkin, E. Koonin, A. Pavlov, N. Pavlova, V. Karamychev, N. Polouchine, V. Shakhova, I. Grigoriev, Y. Lou, D. Rohksar, S. Lucas, K. Huang, D. M. Goodstein, T. Hawkins, V. Plengvidhya, D. Welker, J. Hughes, Y. Goh, A. Benson, K. Baldwin, J. H. Lee, I. Diaz-Muniz, B. Dosti, V. Smeianov, W. Wechter, R. Barabote, G. Lorca, E. Altermann, R. Barrangou, B. Ganesan, Y. Xie, H. Rawsthorne, D. Tamir, C. Parker, F. Breidt, J. Broadbent, R. Hutkins, D. O'Sullivan, J. Steele, G. Unlu, M. Saier, T. Klaenhammer, P. Richardson, S. Kozyavkin, B. Weimer, and D. Mills.** 2006. Comparative genomics of the lactic acid bacteria. Proc. Natl. Acad. Sci. U. S. A. **103:**15611–15616.
32. **Miot, J., K. Benzerara, M. Obst, A. Kappler, F. Hegler, S. Schadler, C. Bouchez, F. Guyot, and G. Morin.** 2009. Extracellular iron biomineralization by photoautotrophic iron-oxidizing bacteria. Appl. Environ. Microbiol. **75:** 5586–5591.
33. **Orphan, V. J., C. H. House, K. U. Hinrichs, K. D. McKeegan, and E. F. DeLong.** 2001. Methane-consuming archaea revealed by directly coupled isotopic and phylogenetic analysis. Science **293:**484–487.
34. **Pandey, A., F. Bringel, and J. M. Meyer.** 1994. Iron requirement and search for siderophores in lactic acid bacteria. Appl. Microbiol. Biotechnol. **40:**735–739.
35. **Reimer, L., U. Zepke, J. Moesch, S. T. Schulze-Hillert, M. Ross-Messemer, W. Probst, and E. Weimer.** 1992. EELS spectroscopy: a reference handbook of standard data for identification and interpretation of electron energy loss spectra and for generation of electron spectroscopic images. Carl Zeiss, Electron Optics Division, Oberkochen, Germany.
36. **Sebulsky, M. T., D. Hohnstein, M. D. Hunter, and D. E. Heinrichs.** 2000. Identification and characterization of a membrane permease involved in iron-hydroxamate transport in *Staphylococcus aureus*. J. Bacteriol. **182:**4394–4400.
37. **Siezen, R. J., M. J. C. Starrenburg, J. Boekhorst, B. Renckens, D. Molenaar, and J. Vlieg.** 2008. Genome-scale genotype-phenotype matching of two *Lactococcus lactis* isolates from plants identifies mechanisms of adaptation to the plant niche. Appl. Environ. Microbiol. **74:**424–436.
38. **Sinha, A. K.** 1972. Colorimetric assay of catalase. Anal. Biochem. **47:**389–394.
39. **Vannier-Santos, M. A., A. Martiny, U. Lins, J. A. Urbina, V. M. Borges, and W. de Souza.** 1999. Impairment of sterol biosynthesis leads to phosphorus and calcium accumulation in *Leishmania acidocalcisomes*. Microbiology **145:** 3213–3220.
40. **Wandersman, C., and P. Delepelaire.** 2004. Bacterial iron sources: from siderophores to hemophores. Annu. Rev. Microbiol. **58:**611–647.
41. **Weinberg, E. D.** 1997. The *Lactobacillus* anomaly: total iron abstinence. Perspect. Biol. Med. **40:**578–583.